PHYSICAL REVIEW A, VOLUME 63, 033801

Effects of $\chi^{(3)}$ nonlinearities in second-harmonic generation

M. K. Olsen, V. I. Kruglov, and M. J. Collett

Department of Physics, University of Auckland, Private Bag 92019, Auckland, New Zealand

(Received 10 July 2000; published 5 February 2001)

We investigate the effects of higher-order, $\chi^{(3)}$, nonlinearities on the process of second-harmonic generation. In the traveling-wave case we find substantive differences in the macroscopic behavior of the fields when the $\chi^{(3)}$ components are present. In the intracavity case, which has been investigated before using a linearized analysis, we investigate regions where these analyses may not be valid, comparing and contrasting the full quantum simulations with previous results.

DOI: 10.1103/PhysRevA.63.033801 PACS number(s): 42.65.Ky, 42.50.Dv, 42.50.Lc

I. INTRODUCTION

It has long been known that nonlinear parametric processes such as second-harmonic generation (SHG), optical parametric oscillation (OPO), and amplification (OPA) can produce nonclassical states of the electromagnetic field [1]. Much theoretical and experimental work has been done on these cases, in both of which electromagnetic fields at differing frequencies are coupled by a second-order, $\chi^{(2)}$ nonlinearity.

There have also been a number of theoretical analyses of systems in which both $\chi^{(2)}$ and higher-order nonlinearities are present. Gerry and Rodrigues [2] investigated a system of traveling-wave down-conversion with an added $\chi^{(3)}$ anharmonic term. Making the approximation that the pump field was classical and undepleted during the interaction with the nonlinear medium, they predicted squeezing and antibunching effects for short interaction times. Tombesi [3] analyzed a system with two external pumping fields and $\chi^{(2)}$, $\chi^{(3)}$, and $\chi^{(4)}$ nonlinearities. He predicted enhanced quadrature squeezing via reduced interaction length, although he also assumed classical, undepleted pumping. García Fernández *et al.* [4] analyzed the degenerate parametric amplifier with added fourth-order interaction and undepleted classical pumping, using a linearized fluctuation approach.

Cabrillo and Bermejo [5] dropped the undepleted pump approximation to analyze the optical parametric oscillator with a $\chi^{(3)}$ interaction in the low frequency mode only. Using a linearized analysis, they found that even though the quadrature noise in the total field tended to increase, there was a spectral redistribution so that they actually found better squeezing at some frequencies. Cabrillo *et al.* [6] studied the quadrature squeezing and mean fields for an OPA with added $\chi^{(3)}$, using a linearization of Wigner representation stochastic differential equations, again using the undepleted pump approximation. Kryuchkyan and Kheruntsyan [7] used the complex P representation to perform an analysis of a driven OPO with third-order nonlinearity, calculating the effects of the quantum noise on the nonlinear dynamics and quantum statistics of the signal field. They again used a classical pump approximation. Kheruntsyan *et al.* [8] used the complex P representation to calculate the Wigner function for a similar system, but with a quantum treatment of both high and low frequency modes, although only the degenerate low frequency mode was subject to the $\chi^{(3)}$ interaction.

The process of intracavity second-harmonic generation with an added $\chi^{(3)}$ nonlinearity which affects the fundamental mode only has been analyzed by Cabrillo *et al.* [9]. The authors, using a linearized analysis, calculate that the Hopf bifurcation normally found in SHG can be shifted towards higher photon numbers and that, for a high enough value of $\chi^{(3)}$, the system can be completely stabilized. Calculating the quadrature noise spectra, the authors also find a supression of the excess noise in the antisqueezed quadrature, caused by the Kerr nonlinearity. The authors calculate that, for the appropriate combination of parameters, perfect quadrature squeezing can be found at the critical operating point, although a linearized fluctuation analysis is not expected to be fully valid at this point.

Our aim in this work is to perform a fully quantum investigation of the system of SHG with competing $\chi^{(2)}$ and $\chi^{(3)}$ nonlinearities in both modes, using the positive P representation [10] and a linearized fluctuation analysis where appropriate. We wish to calculate how the inclusion of the Kerr nonlinearities may affect the mean fields and the quantum statistics in both the traveling-wave and cavity configurations of second-harmonic generation. In the traveling-wave case we use numerical stochastic integration as it has been shown previously that linearization in the case of pure SHG has limited validity, not even giving the correct solutions for the mean fields [11–13]. In the intracavity case, we use both numerical stochastic integration and, where we can demonstrate its validity, a semianalytical linearization method.

II. TRAVELING-WAVE CASE

We consider a nonlinear $\chi^{(2)}$ and $\chi^{(3)}$ crystal, in which a pump field at frequency ω produces a harmonic field at frequency 2ω. We consider here only the case of perfect phase-matching between the two fields, with both fields considered as plane waves. In the traveling-wave regime we can write an interaction Hamiltonian, with the trivial ω dependence of the fields removed, as

$$\mathcal{H}=\frac{i\hbar\kappa}{2}[\hat{a}^{\dagger 2}\hat{b}-\hat{a}^{2}\hat{b}^{\dagger}]+\hbar\chi[\hat{a}^{\dagger 2}\hat{a}^{2}+\hat{b}^{\dagger 2}\hat{b}^{2}]+2\hbar\chi_{ab}\hat{a}^{\dagger}\hat{a}\hat{b}^{\dagger}\hat{b}, \tag{1}$$

where $\hat{a}$ and $\hat{b}$ are the annihilation operators for photons at frequencies ω and 2ω, respectively, at position z inside the

nonlinear crystal, κ represents the effective strength of the nonlinear interaction between the two modes, χ represents the effective strength of the self-phase modulation $\chi^{(3)}$ nonlinearity, and χ_{ab} represents the strength of the cross-phase modulation $\chi^{(3)}$ nonlinearity. We consider here the case where the Kerr type interaction has equal effective strengths for each mode. The cross phase modulation strength will depend on such things as the mode overlap and can typically vary up to the maximum of the self-interaction strength. The operator equations of motion for the system are found as

$$\frac{d\hat{a}}{dz}=\kappa\hat{a}^{\dagger}\hat{b}-2i\chi\hat{a}^{\dagger}\hat{a}^{2}-2i\chi_{ab}\hat{a}\hat{b}^{\dagger}\hat{b},$$
$$\frac{d\hat{b}}{dz}=-\frac{\kappa}{2}\hat{a}^{2}-2i\chi\hat{b}^{\dagger}\hat{b}^{2}-2i\chi_{ab}\hat{a}^{\dagger}\hat{a}\hat{b}, \tag{2}$$

for which no analytical solution is known.

The first level of approximation often used in solving operator equations is linearization, or assuming that the operators can be directly replaced by complex numbers to give the mean values of the fields. In the case of traveling-wave SHG, this method has been shown to have limited validity [12], but in the present case we find an analytical solution for the photon number which more closely follows the full quantum solutions, at least when we set the cross-phase modulation term χ_{ab} to zero. Making the substitutions $\hat{a}\rightarrow\alpha=\langle\hat{a}\rangle$ and $\hat{b}\rightarrow\beta=\langle\hat{b}\rangle$ gives the following classical equations:

$$\frac{d\alpha}{dz}=-2i\chi|\alpha|^{2}\alpha-2i\chi_{ab}|\beta|^{2}\alpha+\kappa\alpha^{*}\beta,$$
$$\frac{d\beta}{dz}=-2i\chi|\beta|^{2}\beta-2i\chi_{ab}|\alpha|^{2}\beta-\frac{\kappa}{2}\alpha^{2}. \tag{3}$$

Note that we have not bothered with the normal method of calculating fluctuations around the classical solutions, as experience with the pure SHG system has shown the results to be highly inaccurate after a short interaction length and we would expect this to be the case here also.

In this situation, as opposed to the situation of pure traveling-wave SHG, we can find a reasonably accurate analytical solution for the field intensities. After much manipulation (see the Appendix), and setting χ_{ab} to zero, we find an equation of motion for the new variable $x=2\chi[5|\beta(z)|^{2}-2|\alpha(0)|^{2}]$,

$$\frac{dx}{dz}=\pm\sqrt{a_0+a_1x+a_2x^{2}+a_3x^{3}+a_4x^{4}}, \tag{4}$$

where $a_0=2E$, the pseudoenergy obtained by treating d^2x/dz^2 as a pseudoacceleration resulting from a pseudopotential

$$U(x)=-\frac{1}{2}(a_1x+a_2x^{2}+a_3x^{3}+a_4x^{4}), \tag{5}$$

so that $(dx/dz)^2+2U(x)=2E$ is a constant of the motion. In the above equations, defining $C_1=8\chi^2|\alpha(0)|^4$, we also have

$$a_1=-\frac{14\kappa^{2}\chi}{5}C_0^{2},$$
$$a_2=\frac{4}{5}\kappa^{2}C_0+C_1,$$
$$a_3=\frac{2\kappa^{2}}{5\chi}, \tag{6}$$
$$a_4=-\frac{1}{4}.$$

We can now rearrange and integrate Eq. (2) to give

$$z=\pm\int_{x(0)}^{x(z)}\frac{dx}{\sqrt{a_0+a_1x+a_2x^{2}+a_3x^{3}+a_4x^{4}}}, \tag{7}$$

where $x(0)=-4\chi|\alpha(0)|^2$. Using energy conservation, it is clear that any solution for $x(z)$ also implies a solution for $|\alpha(z)|^2$. We find that there are three cases where Eq. (7) has periodic solutions. Defining

$$f(x)=\sum_{k=0}^{4}a_kx^{k},$$
$$=-\lambda^{2}\prod_{k=1}^{4}(x-x_k), \tag{8}$$

where $a_4=-\lambda^2$ and $\lambda>0$, we examine the roots of $f(x)=0$.

In the first two cases, there are four real roots: $x_1>x_2>x_3>x_4$ and the solution can be written as

$$x(z)=M+\frac{N}{D+\mathrm{sn}^{2}(\Omega z+\phi,k)}, \tag{9}$$

where sn is the Jacobi sine amplitude of modulus k [14] and

$$\Omega=\frac{\lambda}{2}\sqrt{(x_1-x_3)(x_2-x_4)},$$
$$k=\sqrt{\frac{(x_1-x_2)(x_3-x_4)}{(x_2-x_4)(x_1-x_3)}}, \tag{10}$$

and the constant ϕ is determined from the initial condition by

$$\phi=\mathrm{sn}^{-1}\left(\sqrt{\frac{N-D[x(0)-M]}{[x(0)-M]}},k\right). \tag{11}$$

The function $x(z)$ is periodic, with the period given by

$$T=\frac{2}{\Omega}\int_0^1 \frac{dt}{\sqrt{(1-t^2)(1-k^2t^2)}}=\frac{2}{\Omega}K(k), \tag{12}$$

where $K(k)$ is the full elliptic integral. It is clear that the period of $x(z)$ is the same as that of $|\alpha(z)|^2$.

We find that there are two separate cases for the solution given by Eq. (9). The first of these cases, which is that encountered for the parameters we have used in this investigation, is where (i) $x_3 \geqslant x \geqslant x_4$: In this case $M=x_1$, $N=-(x_1-x_4)(x_1-x_3)/(x_3-x_4)$, and $D=(x_1-x_3)/(x_3-x_4)$; (ii) $x_1 \geqslant x \geqslant x_2$: In this case, $M=x_4$, $N=(x_1-x_4)(x_2-x_4)/(x_1-x_2)$, and $D=(x_2-x_4)/(x_1-x_2)$. These two cases correspond to motion of a pseudoparticle in the two different branches of a quartic pseudpopotential.

The other type of periodic solution arises when we find two real roots, x_1 and x_2, with $x_1>x_2$, and two complex roots for $f(x)$. Writing

$$f(x)=-\lambda^2(x-x_1)(x-x_2)(x^2-2\mu x+\nu), \tag{13}$$

the solution has the form, for $x_1 \geqslant x \geqslant x_2$,

$$x(z)=M_0+\frac{N_0}{D_0-\mathrm{cn}(\Omega_0 z+\phi_0,k_0)}, \tag{14}$$

where cn signifies the Jacobi cosine amplitude. Defining

$$\begin{aligned} y_1&=\sqrt{x_1^2-2\mu x_1+\nu},\\ y_2&=\sqrt{x_2^2-2\mu x_2+\nu}, \end{aligned} \tag{15}$$

we have

$$M_0=\frac{y_1x_2-y_2x_1}{y_1-y_2},$$

$$N_0=\frac{2y_1y_2(x_1-x_2)}{(y_1-y_2)^2},$$

$$D_0=\frac{y_1+y_2}{y_1-y_2},$$

$$\Omega_0=\lambda\sqrt{y_1y_2},$$

$$k_0=\sqrt{\frac{y_1y_2-x_1x_2+\mu(x_1+x_2)-\nu}{2y_1y_2}},$$

$$\phi_0=\mathrm{cn}^{-1}\left(\frac{D_0[x(0)-M_0]-N_0}{x(0)-M_0},k_0\right). \tag{16}$$

In this case the period of $x(z)$ has the form

$$T_0=\frac{4}{\Omega_0}\int_0^1 \frac{dt}{\sqrt{(1-t^2)(1-k_0^2t^2)}}=\frac{4}{\Omega_0}K(k_0). \tag{17}$$

Solving the classical equations numerically using a fourth and fifth order Runge-Kutta method also shows that the mean-field intensities undergo periodic revivals, as shown in Fig. 1. The horizontal axis is a normalized interaction distance, $\xi=\kappa z|\alpha(0)|/\sqrt{2}$. Note that there is no visible difference in these solutions whether we ignore the effects of the cross-phase modulation or set it to its maximum value, $\chi_{ab}=\chi$. Although interesting in itself when compared with the classical solution for traveling-wave SHG, which does not exhibit any periodicity [15], neither the analytical or numerical solutions of the classical equations allow us to reliably calculate any of the quantum statistics of the two fields. To do this we turn to one of the phase space representations of quantum optics.

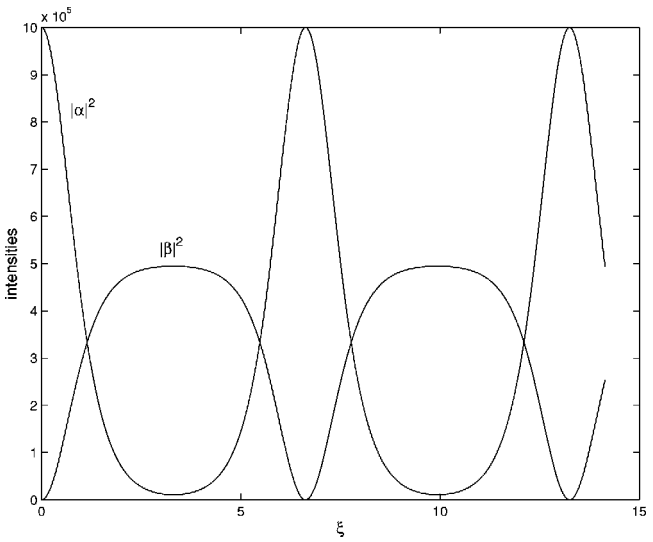

FIG. 1. The classically calculated intensities of the fundamental and harmonic as functions of the normalized interaction distance, ξ, for $|\alpha(0)|^2=10^6$, $\kappa=0.01$, and $\chi=10^{-7}$.

Using the usual methods [16], this system can be mapped exactly onto positive-P equations, via the master and Fokker-Planck equations. For purposes of comparison, we first give the equations with χ_{ab} set to zero, which allows a particularly simple factorization of the diagonal diffusion matrix, giving

$$\begin{aligned} \frac{d\alpha}{dz}&=\kappa\alpha^\dagger\beta-2i\chi\alpha^2\alpha^\dagger+\sqrt{\kappa\beta-2i\chi\alpha^2}\,\eta_1(z),\\ \frac{d\alpha^\dagger}{dz}&=\kappa\alpha\beta^\dagger+2i\chi\alpha^{\dagger\,2}\alpha+\sqrt{\kappa\beta^\dagger+2i\chi\alpha^{\dagger\,2}}\,\eta_2(z),\\ \frac{d\beta}{dz}&=-\frac{\kappa}{2}\alpha^2-2i\chi\beta^2\beta^\dagger+\sqrt{-2i\chi\beta^2}\,\eta_3(z),\\ \frac{d\beta^\dagger}{dz}&=-\frac{\kappa}{2}\alpha^{\dagger\,2}+2i\chi\beta^{\dagger\,2}\beta+\sqrt{2i\chi\beta^{\dagger\,2}}\,\eta_4(z). \end{aligned} \tag{18}$$

In the above system of equations, there is a correspondence between $[\hat{a},\hat{a}^\dagger,\hat{b},\hat{b}^\dagger]$ and $[\alpha,\alpha^\dagger,\beta,\beta^\dagger]$, although the latter are c-number variables that are not complex conjugate except in the mean of a large number of stochastic trajectories. This is due to the independence of the real noise terms, which

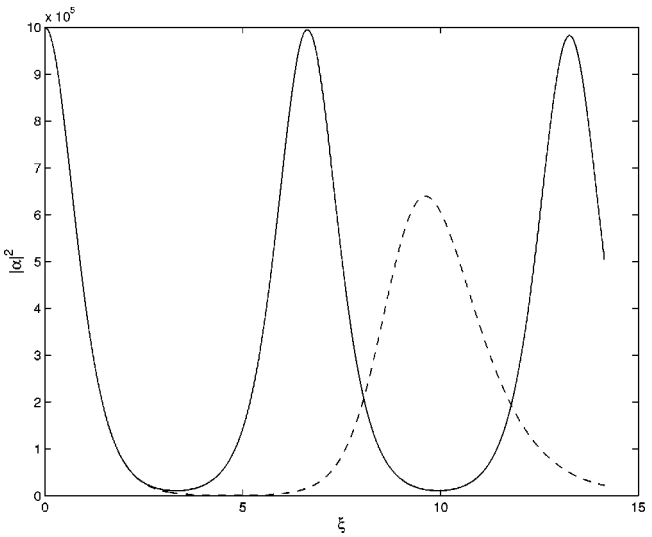

FIG. 2. The intensities of the fundamental and harmonic as functions of the normalized interaction distance, ξ, for $|\alpha(0)|^2=10^6$, $\kappa=0.01$, and $\chi=10^{-7}$, calculated using the positive P representation. The dotted lines are for $\chi=0$, the case of pure second-harmonic generation.

have the properties $\overline{\eta_j(z)}=0$ and $\overline{\eta_i(z)\,\eta_j(z')}=\delta_{ij}\delta(z-z')$. The positive P equations can then be numerically integrated to calculate not only the mean-field behavior, but also the quantum statistics of the fields. The mean-field intensities, calculated using 10^5 stochastic trajectories, are shown in Fig. 2 for an initial photon number in the fundamental of $\langle\hat{a}^\dagger\hat{a}\rangle=10^6$ and nonlinearities of $\kappa=0.01$ and $\chi=10^{-7}$, a ratio which is realistic for many materials. We can readily see that, unlike the case of pure SHG, the behavior is close to that found classically.

In this case we are also interested in the quadrature variances, as unusual behavior has previously been found in the pure $\chi^{(2)}$ case. Defining the quadratures by

$$X_\theta=a\mathrm{e}^{-i\theta}+a^\dagger\mathrm{e}^{i\theta}, \tag{19}$$

we see that the coherent state value for any quadrature variance is equal to 1. The X_0 quadrature variances for the fundamental and harmonic are shown in Fig. 3, with the same quantities for pure SHG shown by dotted lines. It can immediately be seen that the maximum obtainable squeezing is less when the $\chi^{(3)}$ interaction is included, with the squeezing being available over a smaller interaction length. This change in the statistics of the fields, from squeezed to highly antisqueezed, is explained by the spontaneous nature of the downconversion process as energy is transferred back from the harmonic to the fundamental.

One interesting question with the present system is whether other quadratures at different θ may exhibit better squeezing for different interaction lengths. After all, the $\chi^{(3)}$ term essentially operates on the phase of the fields and could well produce a quadrature rotation effect. This quadrature rotation effect is apparent in simulations, with the variances for different θ actually crossing at different interaction lengths, but is such a small effect for the parameters that we have used that it only happens well after the squeezing has essentially disappeared. This means that even though the minimum noise is found in a different quadrature, this quadrature never exhibits better squeezing than X_0 around $\xi\approx 2\rightarrow 3$. The variances in the fundamental are shown for various quadratures in Fig. 4.

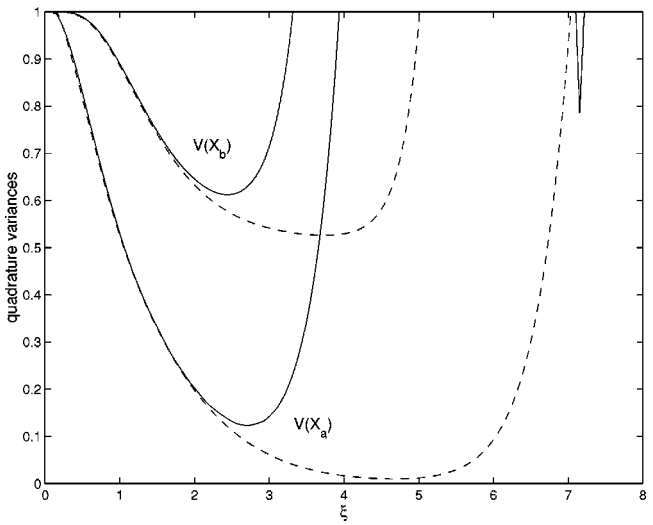

FIG. 3. The X quadrature variances for the traveling-wave case in the fundamental and harmonic, calculated using 10^5 stochastic trajectories. The parameters are the same as in Fig. 2. The variances for pure SHG are shown by the dotted lines.

Effect of cross-phase modulation

Although the inclusion of what we would expect to be the maximum value of the cross-phase term made no visible difference to the mean fields, it is still of interest to investigate what effect it may have on the quantum statistics of the two fields. Proceeding as above, we find that the positive-P

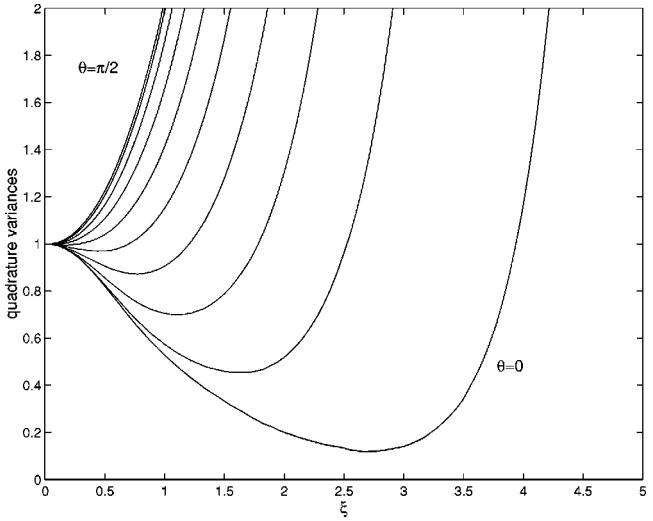

FIG. 4. The X_θ quadrature variances for the traveling-wave case in the fundamental, calculated using 10^5 stochastic trajectories. The θ values are equally spaced from 0 to $\pi/2$. It can be seen that the maximum squeezing is found for $\theta=0$.

Fokker-Planck equation for the system no longer has a diagonal diffusion matrix, which means that no simple and obvious factorization resulting in the stochastic differential equations suggests itself. However, the factorization we have chosen (which is by no means unique), leads to the following system of stochastic equations:

$$\frac{d\alpha}{dz}=\kappa\alpha^{\dagger}\beta-2i\chi\alpha^{2}\alpha^{\dagger}-2i\chi_{ab}\alpha\beta^{\dagger}\beta+\sqrt{\frac{-2i}{\chi}}\chi_{ab}\alpha\eta_1(z)+\sqrt{\kappa\beta-2i\alpha^{2}(\chi-\chi_{ab}^{2}/\chi)}\eta_3(z),$$

$$\frac{d\alpha^{\dagger}}{dz}=\kappa\alpha\beta^{\dagger}+2i\chi\alpha^{\dagger\,2}\alpha+2i\chi_{ab}\alpha^{\dagger}\beta^{\dagger}\beta+\sqrt{\frac{2i}{\chi}}\chi_{ab}\alpha^{\dagger}\eta_2(z)+\sqrt{\kappa\beta^{\dagger}+2i\alpha^{\dagger\,2}(\chi-\chi_{ab}^{2}/\chi)}\eta_4(z), \tag{20}$$

$$\frac{d\beta}{dz}=-\frac{\kappa}{2}\alpha^{2}-2i\chi\beta^{2}\beta^{\dagger}-2i\chi_{ab}\alpha^{\dagger}\alpha\beta+\sqrt{-2i\chi\beta^{2}}\eta_1(z),$$

$$\frac{d\beta^{\dagger}}{dz}=-\frac{\kappa}{2}\alpha^{\dagger\,2}+2i\chi\beta^{\dagger\,2}\beta+2i\chi_{ab}\alpha^{\dagger}\alpha\beta^{\dagger}+\sqrt{2i\chi\beta^{\dagger\,2}}\eta_2(z),$$

where all variables and noises are defined as in Eq. (18).

From numerical integration of these equations we find that the intensities of the two fields are not noticeably changed, whether $\chi_{ab}=0$ or is equal to χ. In parameter regions where quadrature noise reduction is found with no cross-phase modulation present, the addition of the maximum χ_{ab} value does not perceptibly change the squeezing found. However, for the quadrature angles and regimes which exhibit excess noise, the maximum cross-phase modulation can increase this noise by a factor of approximately 10%.

III. INTRACAVITY CASE

The case of intracavity SHG with added $\chi^{(3)}$ interaction has been previously examined in the case where this interaction affects only the fundamental mode [9]. This analysis also used a linearized fluctuation analysis about the steady state values of the fields. Here we wish to include the higher order nonlinearity in both the modes and calculate the field statistics without necessarily using the linearization approach. We also compare noise spectra calculated in the linearized approach with those obtained by stochastic integration of the full quantum equations. We will first investigate the case without cross-phase modulation, where $\chi_{ab}=0$.

With a cavity, the positive *P*-representation equations are

$$\frac{d\alpha}{dt}=\epsilon-\gamma_1\alpha+\kappa\alpha^{\dagger}\beta-2i\chi\alpha^{2}\alpha^{\dagger}+\sqrt{\kappa\beta-2i\chi\alpha^{2}}\eta_1(t),$$

$$\frac{d\alpha^{\dagger}}{dt}=\epsilon^{*}-\gamma_1\alpha^{\dagger}+\kappa\alpha\beta^{\dagger}+2i\chi\alpha^{\dagger\,2}\alpha+\sqrt{\kappa\beta^{\dagger}+2i\chi\alpha^{\dagger\,2}}\eta_t(z), \tag{21}$$

$$\frac{d\beta}{dt}=-\gamma_2\beta-\frac{\kappa}{2}\alpha^{2}-2i\chi\beta^{2}\beta^{\dagger}+\sqrt{-2i\chi\beta^{2}}\eta_3(t),$$

$$\frac{d\beta^{\dagger}}{dt}=-\gamma_2\beta^{\dagger}-\frac{\kappa}{2}\alpha^{\dagger\,2}+2i\chi\beta^{\dagger\,2}\beta+\sqrt{2i\chi\beta^{\dagger\,2}}\eta_4(t).$$

In the above, we have assumed phase matching without the $\chi^{(3)}$ terms and the γ_j are the cavity loss rates at each frequency, while ϵ represents the classical pumping field at the lower frequency. The noise terms are as before, except that they are now δ correlated in time rather than in space. In our calculations we will always set $\gamma_1=\gamma_2=1$.

In normal SHG, it is well known that a Hopf bifurcation exists at a critical pumping strength, $\epsilon_c=(1/\kappa)(\gamma_2+2\gamma_1)\sqrt{2\gamma_2(\gamma_1+\gamma_2)}$ [17,18]. It is normally assumed that a linearized fluctuation analysis can be performed below this critical point, which is found by writing operators as the sum of a classical, mean value part and a fluctuations operator, e.g., $\hat{a}=\alpha+\delta\hat{a}$, where it is assumed that $\delta\hat{a}$ is somehow small compared to α. This allows equations to be written for the fluctuation operators in the form of an Ornstein-Uhlenbeck process, allowing easy calculation of the noise spectra. The critical point is actually found by examining the eigenvalues of the drift matrix in the equation for the fluctuations. As long as these do not have a positive real part, the solutions will be stable, although this process in itself says nothing about the size of the fluctuations, nor does it say how accurately equations thus solved will give the quantum statistics of the fields.

Crucial to this stability analysis is the ability to obtain classical steady state solutions to the system obtained by dropping the noise terms in Eq. (21). With standard SHG, this process is trivial and with the $\chi^{(3)}$ interacting only with the fundamental, it is also easy. In our case, however, we use a perturbation expansion, writing

$$\alpha_{ss}=\alpha_0+\chi\alpha_1+\chi^{2}\alpha_2+\cdots,$$
$$\beta_{ss}=\beta_0+\chi\beta_1+\chi^{2}\beta_2+\cdots, \tag{22}$$

where α_0 and β_0 are the steady state solutions to the classical equations with $\chi=0$. With phase matching, $\gamma_1=\gamma_2=\gamma$ and a real pump, we find that α_0 is the real solution of

$$\frac{\kappa^{2}}{2\gamma}\alpha_0^{3}+\gamma\alpha_0+\epsilon=0, \tag{23}$$

and $\beta_0=-\kappa\alpha_0^{2}/2\gamma$. As χ much smaller than the other parameters we will only take our perturbation expansion to first order. This leads to the solutions

$$\beta_{ss}=\beta_0-\frac{2i\chi A}{\kappa\alpha_0+\dfrac{\gamma^{2}}{\kappa\alpha_0}+\gamma\dfrac{\beta_0}{\alpha_0}}, \tag{24}$$

where

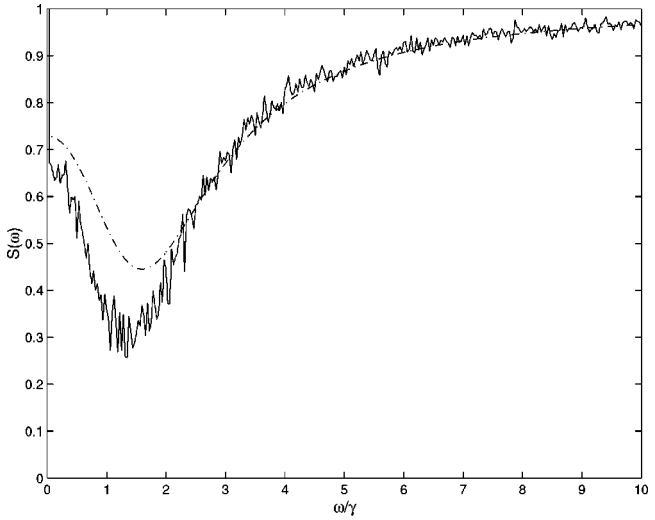

FIG. 5. The X_0 fundamental quadrature variances for the cavity case with $\epsilon=0.4\epsilon_c$. The dash-dotted line is the linearized variance and the full line is the result of stochastic integration, both for $\chi=10^{-7}$. For these parameters there is no visible difference for pure SHG.

$$A=\frac{\beta_0^4}{\alpha_0}-\alpha_0^3+\frac{\gamma\beta_0^3}{\kappa\alpha_0} \tag{25}$$

and

$$\alpha_{ss}=\alpha_0-\frac{\chi}{\kappa\alpha_0}(\gamma\beta_1+2i\beta_0^3). \tag{26}$$

It can be seen from the above expressions that, to first order, the effect of the Kerr nonlinearity is to add an imaginary component to the two field amplitudes.

The steady state solutions thus obtained are then used to perform a numerical stability analysis of the system. We find that, for the values we use here, there is still a Hopf bifurcation so that above a certain critical pumping amplitude, we expect self-pulsing behavior analogous to that found in pure SHG. Our approach here is slightly different from that of Cabrillo *et al.* [9], who define the critical point in terms of a normalized photon number in the fundamental mode. We feel that a definition in terms of pump amplitude should be more experimentally useful. For small values of χ, we find that the critical pumping parameter found from our first-order expansion is little changed from that found for pure SHG.

A. Below the critical point

Below the critical point is where linearization should be most valid, enabling us to calculate steady state noise spectra by treating our system as an Ornstein-Uhlenbeck process [19], using our first-order perturbative solutions as the steady states. We find that, as shown in Fig. 5, that $S(\omega)$ for the X_0 quadrature is effectively unchanged at $\epsilon=0.4\epsilon_c$ for our parameters of $\kappa=0.01$ and $\chi=10^{-7}$, the plotted spectra being indistinguishable on the scale we use.

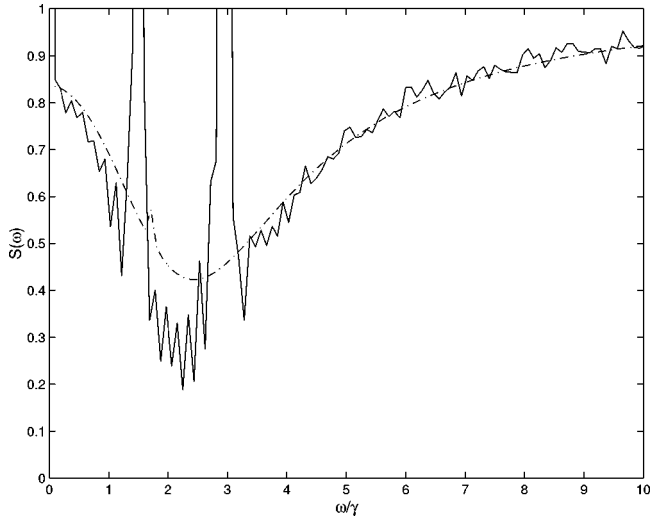

FIG. 6. The X_0 fundamental quadrature variances for the cavity case at the critical point. The full line is the result of 10^5 stochastic trajectories and the dash-dotted line is the linearized variance, both with $\chi=10^{-7}$.

For purposes of comparison and verification of the linearized spectra, we have also calculated $S(\omega)$ stochastically, as the Fourier transform of the mean value of the normally ordered two-time covariance of the X_0 quadrature, taken over 10^5 trajectories of the positive P equations,

$$S(\omega)=1+\mathcal{F}T\langle:X_0(t),X_0(t+\tau):\rangle. \tag{27}$$

As we can only numerically integrate the equations over a finite time interval, we would expect our numerical solution to be most accurate for higher frequencies, as is shown in Fig. 5. We also find that achieving a smooth noise spectrum by stochastic integration requires more trajectories than a smooth mean for $V(X_0)$ in the time domain. What we can see here, however, is that the two methods are in reasonable agreement, with no new features of the spectrum appearing in the stochastic result.

B. At the critical point

When the cavity is pumped at the critical rate we would expect any linearized analysis to have lost validity, whereas stochastic integration remains valid, given the factors of finite integration time and finite number of trajectories mentioned above. We have again used both methods of calculating the spectra, with all parameters unchanged except for the pump amplitude. In Fig. 6, we show the linearized and stochastic results with the $\chi^{(3)}$ component present. We can readily see that the stochastically calculated spectrum has two large spikes of excess noise, at $\omega\approx\sqrt{3}$ and $\omega\approx 3$. The lower frequency spike is hinted at in the linearized result, but is much smaller and at a slightly higher frequency. This spike is at the frequency of the purely imaginary eigenvalues of the linearized fluctuations matrix [18], $\omega\approx\sqrt{3}$ for our parameters. This lower frequency spike is a signature of the $\chi^{(3)}$ component, not being present in the pure SHG results at the critical point, as we can see in Fig. 7. This figure shows

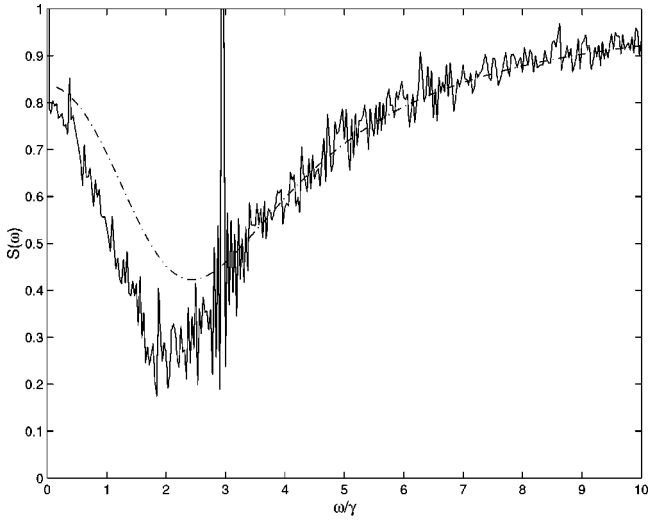

FIG. 7. The X_0 fundamental quadrature variances for pure intracavity SHG at the critical point. The full line is the result of 10^5 stochastic trajectories and the dash-dotted line is the linearized variance.

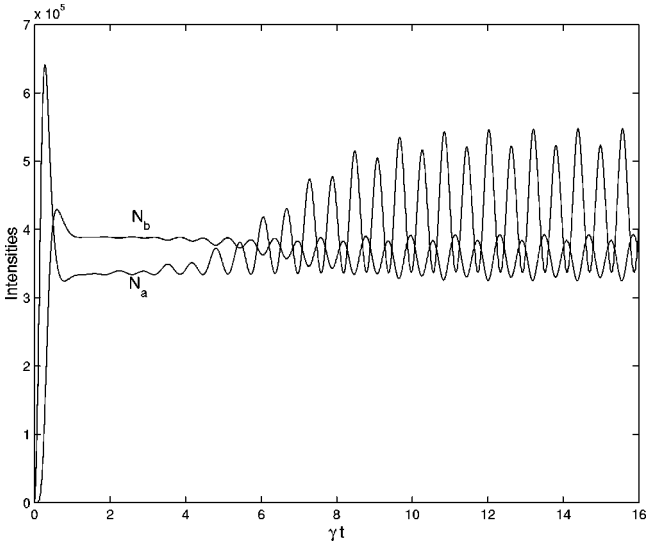

FIG. 8. The mean fields for $\epsilon = 1.2\epsilon_c$, showing the self-pulsing behavior. This is the stochastic solution for 10^5 trajectories $\chi = 10^{-7}$. The classical solution is not visibly different at this scale.

a narrower spike at the higher frequency, but absolutely no new structure in the linearized spectrum. The spikes at the higher frequency seem to be related to an oscillation in the quadrature variance which is not actually visible in the time plots until a higher pump power is used. This is typical of soft-mode oscillations, which will show up in the two-time correlation function in the frequency domain before they are visible in the time domain.

What is of interest in both these figures is that the positive *P* spectra and the linearized spectra are still in broad agreement, despite being at the critical point. However, from time domain integrations we saw that the variances at any other quadrature angle tended to increase with time, with only the X_0 quadrature showing steady state squeezing. This is another feature that is not found in a linearized analysis. We should note here that our calculations do not use the parameters that others have used to predict nearly perfect quadrature squeezing at the critical point, with one cavity loss rate much larger than the other [20], as we are more interested in looking for signatures and effects of the $\chi^{(3)}$ component than in perfecting the squeezing.

C. Above the critical point

As expected, above the critical point we find self-pulsing behavior, as shown in Fig. 8, calculated for $\epsilon = 1.2\epsilon_c$. Again the semiclassical solutions for the mean fields are almost indistinguishable from those obtained using the positive *P*. The pulsing behavior is different to that of pure SHG, with the oscillations beginning earlier and having a greater amplitude and lower frequency, although the time-averaged values for the intensities are almost identical. With $\chi^{(3)}$ we also see oscillations with two different amplitudes, another feature not seen in pure SHG.

When we examine the quadrature variances, we see that the X_0 quadrature displays transient squeezing as shown in Fig. 9, but soon develops excess noise, as shown in Fig. 10. This excess noise is actually less than that found with pure SHG, showing that the $\chi^{(3)}$ component has to some extent stabilized the fields by comparison. The other quadrature angles also all display excess noise as the time increases. This tells us that, as there are no steady state squeezing effects, we would not expect to see very much quadrature squeezing in the frequency domain.

Previously published analytical calculations [21], obtained by a linearization around the periodic solutions for pure SHG in the self-pulsing regime, suggest that intensity squeezing may be found in this regime. These results also show a huge first-order correction to the amplitude spectrum, hinting that amplitude quadrature squeezing is possibly not observable above the critical point.

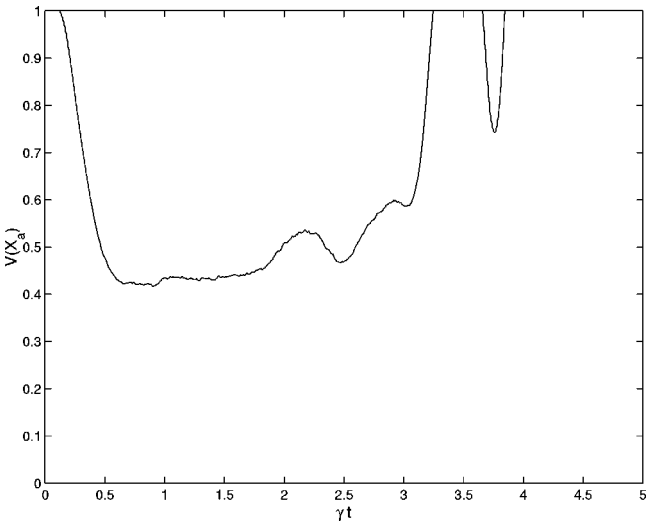

FIG. 9. Short time behavior of the variance in the X_0 quadrature of the fundamental, for $\epsilon = 1.2\epsilon_c$ and $\chi = 10^{-7}$. We can see that squeezing is only a transient effect in this situation.

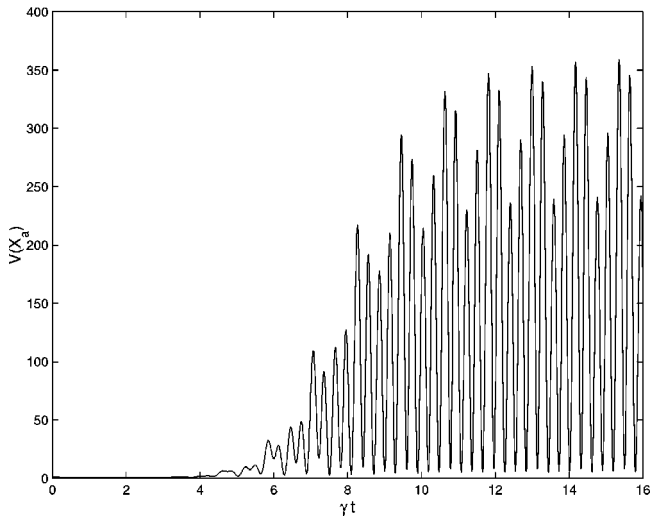

FIG. 10. Longer time behavior of the variance in the X_0 quadrature of the fundamental, for $\epsilon = 1.2\epsilon_c$ and $\chi = 10^{-7}$. The noise increases and becomes periodic as the self-pulsing begins. It is easily seen that there will be no steady state squeezing in this quadrature.

D. Cross-phase modulation in the cavity

Well below the critical point we do not find any noticeable differences in the behavior of the system when we include our maximum value of χ_{ab}, either in the positive P simulations or in linearized results, again performed using a perturbation expansion to first order. However, as we increase the pump power so as to approach the usual critical point (with $\chi^{(2)}$ only), we find that the low frequency spike in the X_a quadrature noise spectrum begins to appear earlier. When we use the normal critical pumping, the spike is much more pronounced, but at the same frequency. Stochastic integration also shows this spike as more pronounced and appearing at a lower pump power than with self-phase modulation only. This is a strong indication that the critical point has moved, although a linearized fluctuation analysis to first order in χ does not show any significant change. This indicates that linearization is not as trustworthy with the cross-phase terms included and we must resort to stochastic integration at lower pumping than for pure $\chi^{(2)}$, or with just the inclusion of the self-phase modulation. We plan to further investigate both the noise properties and the effects of the cross-phase modulation near and above the critical point as part of a more general study into the limits and applicability of linearization.

IV. CONCLUSION

We have analyzed second-harmonic generation in the case where the nonlinear crystal has added $\chi^{(3)}$ nonlinearities. In the traveling-wave case we find marked differences between the dynamic behavior of the fields with and without the $\chi^{(3)}$ components. As far as the quantum statistics of the fields are concerned, we find that less squeezing is achievable in the $\chi^{(3)}$ case. The behavior of the fields is not significantly changed by the inclusion of cross-phase modulation terms.

When we investigate the intracavity situation, we find that the behaviors are essentially the same below the critical point. The amount by which the critical point is changed depends on whether cross-phase modulation is included or not. At and above the critical point, however, we find obvious signatures of the $\chi^{(3)}$ components. Although the Hopf bifurcation is not moved very much, the self-pulsing behavior is quite different. A new oscillation with two distinct amplitudes emerges, with a period significantly larger than that found for pure SHG.

As all materials have some $\chi^{(3)}$ component, and the ratio of $\chi^{(3)}/\chi^{(2)}$ that we have used is rather small, but typical of nonlinear media, it is of interest to know what the signatures of this component are. We have found several signatures that should be accessible to experimental observation.

ACKNOWLEDGMENTS

This research was supported by the University of Auckland Research Committee and the Marsden Fund of the Royal Society of New Zealand. Useful contributions by S. M. Tan are gratefully acknowledged.

APPENDIX: DERIVATION OF ANALYTICAL SOLUTION

Using the fact that $|\alpha(z)|^2 + 2|\beta(z)|^2 = C_0$ is constant in the propagation, in our case being equal to $|\alpha(0)|^2$ and defining $a(z) = |\alpha(z)|^2$, $b(z) = |\beta(z)|^2$ (note that these are not the operators $\hat{a}$ and $\hat{b}$), we find that

$$\frac{da}{dz} = \kappa V,$$
$$\frac{db}{dz} = -\frac{\kappa}{2} V, \tag{A1}$$

where $V = \alpha^{*2}\beta + \alpha^2\beta^*$. Defining also $W(z) = i(\alpha^{*2}\beta - \alpha^2\beta^*)$, we find

$$\frac{dV}{dz} = \kappa a(4b - a) + 2\chi(2a - b)W,$$
$$\frac{dW}{dz} = 2\chi(b - 2a)V. \tag{A2}$$

We now introduce the variable

$$x = 2\chi[5|\beta(z)|^2 - 2|\alpha(0)|^2], \tag{A3}$$

so that we can write

$$\frac{dx}{dz} = -gV,$$
$$\frac{dW}{dz} = Vx, \tag{A4}$$
$$\frac{dV}{dz} = \alpha_0 - \alpha_1 x - \alpha_2 x^2 - Wx,$$

where $g=5\kappa\chi$, $\alpha_0=7\kappa C_0^2/25$, $\alpha_1=4\kappa C_0/25\chi$, and $\alpha_2=3\kappa/25\chi^2$. We now define another constant of the motion,

$$C_1=\frac{1}{2}x^2(z)+gW(z)=8\chi^2|\alpha(0)|^4, \tag{A5}$$

so that we can now write

$$\frac{d^2x}{dz^2}=-\alpha_0 g+(C_1+\alpha_1 g)x+\alpha_2 g x^2-\frac{1}{2}x^3. \tag{A6}$$

Treating d^2x/dz^2 as a pseudoacceleration and $U(x)$ as a pseudopotential, we can write

$$\frac{d^2x}{dz^2}=-\frac{\partial U(x)}{\partial x}, \tag{A7}$$

which leads to

$$\frac{dx}{dz}\cdot\frac{d^2x}{dz^2}=-\frac{dx}{dz}\frac{\partial U(x)}{\partial x}, \tag{A8}$$

or

$$\frac{d}{dz}\left[\frac{1}{2}\left(\frac{dx}{dz}\right)^2\right]=-\frac{dU}{dz}. \tag{A9}$$

From the above equation we can see that $\frac{1}{2}(dx/dz)^2+U(x)$ is a constant, which leads immediately to Eq. (4).

[1] See, for example, *Nonclassical Effects in Quantum Optics*, edited by P. Meystre and D.F. Walls (AIP, New York, 1991).
[2] C.C. Gerry and S. Rodrigues, Phys. Rev. A **36**, 5444 (1987).
[3] P. Tombesi, Phys. Rev. A **39**, 4288 (1989).
[4] P. García Fernández, P. Colet, R. Toral, M. San Miguel, and F.J. Bermejo, Phys. Rev. A **43**, 4923 (1991).
[5] C. Cabrillo and F.J. Bermejo, Phys. Lett. A **170**, 300 (1992).
[6] C. Cabrillo, F.J. Bermejo, P. García Fernández, R. Toral, P. Colet, and M. San Miguel, Phys. Rev. A **45**, 3216 (1992).
[7] G.Yu. Kryuchkyan and K.V. Kheruntsyan, Opt. Commun. **127**, 230 (1996).
[8] K.V. Kheruntsyan, D.S. Krähmer, G.Yu. Kryuchkyan, and K.G. Petrossian, Opt. Commun. **139**, 157 (1997).
[9] C. Cabrillo, J.L. Roldán, and P. García Fernández, Phys. Rev. A **56**, 5131 (1997).
[10] P.D. Drummond and C.W. Gardiner, J. Phys. A **13**, 2353 (1980).
[11] M.K. Olsen and R.J. Horowicz, Opt. Commun. **168**, 135 (1999).
[12] M.K. Olsen, R.J. Horowicz, L.I. Plimak, N. Treps, and C.S. Fabre, Phys. Rev. A **61**, 021803(R) (2000).
[13] M.K. Olsen, L.I. Plimak, M.J. Collett, and D.F. Walls, Phys. Rev. A **62**, 023802 (2000).
[14] I. Gradshtein and I. Ryzhik, *Table of Integrals, Series and Products* (Academic Press, New York, 1994).
[15] J.A. Armstrong, N. Bloembergen, J. Ducuing, and P.S. Pershan, Phys. Rev. **127**, 1918 (1962).
[16] C.W. Gardiner, *Quantum Noise* (Springer-Verlag, Berlin, 1991).
[17] H. Haken and H. Ohno, Opt. Commun. **16**, 205 (1976).
[18] K.J. McNeil, P.D. Drummond, and D.F. Walls, Opt. Commun. **27**, 292 (1978).
[19] C.W. Gardiner, *Handbook of Stochastic Methods* (Springer-Verlag, Berlin, 1985).
[20] M.J. Collett and D.F. Walls, Phys. Rev. A **32**, 2887 (1985).
[21] N.P. Pettiaux, P. Mandel, and C. Fabre, Phys. Rev. Lett. **66**, 1838 (1991).